IMPACT OF MODEL COMPLEXITY ON ACOUSTIC SOURCE LOCALIZATION ACCURACY

M. N. Albezzawy[1,2], G. Chardon[2], H. Demontis[1], J. Picheral[2]

[1] DAAA, ONERA, Institut Polytechnique de Paris, 92320 Châtillon, France
[2] Université Paris-Saclay, CNRS, CentraleSupélec, Laboratoire des signaux et systèmes, 91190 Gif-Sur-Yvette, France

This contribution has been accepted based on the submitted abstract. The submitted manuscript was not reviewed and is reproduced here without edits or corrections by the conference board. Neither the EAA nor the AAA take responsibility for its contents.

Abstract

This paper investigates the limits of acoustic source localization when using multipole-based models in a two-dimensional cylindrical-wave framework. A small candidate displacement of a monopole source relative to the microphone array generates additional spatial patterns beyond the basic monopole field. These patterns carry essential information about the source position. When the source position and multipole amplitudes are estimated jointly from noisy measurements, including more multipole components can unintentionally remove part of this localization information. Dipole and quadrupole terms may absorb the effects of this small displacement, making the position increasingly difficult to identify. This leads to a loss of local identifiability and a degradation of estimation accuracy. More generally, the estimation behavior is governed by the lowest-order residual term in the field expansion. After profiling the fitted multipole amplitudes, the resulting local behavior is analogous to scalar Gaussian mean models with linear, quadratic, or cubic means. These results are derived analytically and confirmed through numerical simulations, showing strong agreement between theory and practice.

Keywords: *source localization, multipolar expansion, estimation accuracy, singular fisher information, cramér-rao bound*

1. Introduction

Acoustic source localization is a fundamental problem in acoustics [1], aeroacoustics [2], room acoustics [3], noise, vibration and harshness applications [4], and structural health monitoring [5]. The objective is to estimate the position of a sound source from measurements collected by an array of sensors. In many practical situations, however, the source is not purely omnidirectional. Its radiation pattern may be directional and is often represented using multipole components such as monopoles, dipoles, quadrupoles, and higher-order terms [6].

This leads to a joint estimation problem where the source position and the source directivity must be estimated simultaneously. In a multipole formulation, the directivity is represented by unknown multipole amplitudes. These amplitudes act as nuisance parameters when the main quantity of interest is the source position. Although adding multipole components improves the ability of the model to represent complex radiation patterns, it can also make localization more difficult [6].

The difficulty comes from the fact that a small displacement of a source of a given order, for example a monopole, generates field variations that have the same spatial structure as higher-order multipole components, such as dipoles and quadrupoles. Consequently, when multipole amplitudes are estimated freely, part of the information associated with source displacement can be absorbed by the directivity parameters. This creates a coupling between localization and directivity estimation and may lead to a loss of local identifiability due to a singular Fisher information matrix [6]. In other words, a directivity component fitted at one assumed position may mimic the field variation that would otherwise reveal a small displacement of a simpler source.

In this work, we study this mechanism in a two-dimensional cylindrical-wave framework. The analysis is performed locally around a reference position, chosen as the origin. The parameter (x) is therefore interpreted as a candidate displacement around this reference position. The field generated by a candidate monopole located at (x,0) is expanded around the origin in order to identify the harmonic terms created by this displacement. In the singular analysis and in the numerical simulations, the true source is located

Corresponding author: *muhammad.albezzawy@onera.fr.*

at the reference position, while the likelihood is evaluated over a grid of candidate positions around the reference position.

We then analyze three truncated estimation models: monopole only, monopole plus dipole, and monopole plus dipole plus quadrupole. For each model, we determine analytically which displacement-induced terms are absorbed by the fitted multipole amplitudes and which residual term remains available for localization. This approach allows us to characterize the interplay between source position and multipole amplitudes and to understand how model complexity influences localization performance. The analytical findings are then confirmed by numerical simulations.

The source model and the three truncated estimation models are introduced in Section 2. Their effect on local identifiability and localization accuracy is then analyzed. The analytical findings are validated by numerical simulations in Section 3. Conclusions are finally given in Section 4.

2. Acoustic model and truncated representations

We consider a two-dimensional monopole source whose candidate position is $(x, 0)$, where x denotes a local displacement with respect to a fixed reference position chosen as the origin. For a fixed observation point (X, Y), the acoustic pressure field associated with this candidate position is

$$u_x(X,Y) = AH_0\left(k\rho_x\right), \tag{1}$$

where

$$\rho_x = \sqrt{(X-x)^2 + Y^2}. \tag{2}$$

Here, A is the monopole amplitude, k is the acoustic wavenumber, and H_ℓ denotes the Hankel function of the first kind of order ℓ (with $\ell = 0$ for a monopole). The case $x = 0$ corresponds to the source located at the reference position.

To derive a local expansion with respect to the source displacement, we fix the observation point (X, Y) and define the auxiliary function

$$g(s) = AH_0\left(k\sqrt{(X-s)^2 + Y^2}\right). \tag{3}$$

The acoustic field when the source is at the origin, i.e. when $x = 0$, is denoted by $u_0(X, Y)$. It is given by

$$u_0(X,Y) = AH_0\left(k\sqrt{X^2 + Y^2}\right). \tag{4}$$

With this notation, we have

$$g(0) = u_0(X,Y), \qquad g(x) = u_x(X,Y). \tag{5}$$

Applying the Taylor expansion of g around $s = 0$ gives

$$g(x) = g(0) + g'(0)x + \frac{g''(0)}{2}x^2 + \frac{g^{(3)}(0)}{6}x^3 + O(x^4). \tag{6}$$

We introduce the polar coordinates centered at the fixed origin,

$$r = \sqrt{X^2 + Y^2}, \qquad \theta = \operatorname{atan2}(Y, X). \tag{7}$$

After calculating $g'(0)$, $g''(0)$, and $g^{(3)}(0)$, the shifted candidate monopole field can be written as

$$u_x = c_0(x)\psi_0 + c_1(x)\psi_1 + c_2(x)\psi_2 + c_3(x)\psi_3 + O(x^4). \tag{8}$$

The origin-centered harmonic components are defined by

$$\psi_0 = H_0(kr), \qquad \psi_1 = \cos\theta\, H_1(kr), \tag{9}$$

and

$$\psi_2 = \cos(2\theta)\, H_2(kr), \qquad \psi_3 = \cos(3\theta)\, H_3(kr). \tag{10}$$

The first coefficients are

$$c_0(x) = A\left(1 - \frac{k^2x^2}{4}\right), \tag{11}$$

$$c_1(x) = A\left(kx - \frac{k^3x^3}{8}\right), \tag{12}$$

$$c_2(x) = A\frac{k^2x^2}{4}, \tag{13}$$

and

$$c_3(x) = A\frac{k^3x^3}{24}. \tag{14}$$

For clarity, the analytical derivation is written using real cosine harmonics. This choice is natural because the candidate displacement is taken along the x-axis, so the local expansion of the field generates cosine angular dependencies. The same subspaces can equivalently be represented using complex exponential harmonics with positive and negative orders, since

$$\cos(\ell\theta) = \frac{e^{i\ell\theta} + e^{-i\ell\theta}}{2}. \tag{15}$$

The real angular basis is therefore used only to simplify the analytical presentation.

The basis functions ψ_j depend only on the fixed observation coordinates. The source displacement x appears only in the coefficients $c_j(x)$. Because the analysis is local around $x = 0$, the first non-zero residual term dominates the small-displacement behavior, while higher-order terms are asymptotically negligible. Therefore, as follows from Eqs. (12) to (14), a small candidate displacement of a monopole source generates a hierarchy of harmonic components: a dipole term proportional to x, a quadrupole term proportional to x^2, and an octupole term proportional to x^3.

2.1. Truncated directivity models

We now consider three truncated directivity models. In each case, the included multipole amplitudes are estimated jointly with the source position. Assuming additive Gaussian noise, maximum likelihood estimation is equivalent to a least-squares fitting problem.

For a model containing the first q harmonic components, we write

$$m_q = \sum_{\ell=0}^{q-1} a_\ell \psi_\ell. \tag{16}$$

Here, a_ℓ are unknown fitted amplitudes. For a fixed candidate displacement x, the noiseless field is

$$u_x = \sum_{\ell=0}^{\infty} c_\ell(x)\psi_\ell. \tag{17}$$

In the least-squares projection, the fitted amplitudes absorb the components that belong to the chosen model. In the noiseless case, this gives

$$a_\ell = c_\ell(x), \qquad \ell = 0, \ldots, q-1. \tag{18}$$

Therefore, after profiling the amplitudes, the information about x carried by the fitted coefficients is no longer independently available for localization. The source position can then only be inferred from the residual field

$$R_q(x) = u_x - m_q. \tag{19}$$

Equivalently,

$$R_q(x) = \sum_{\ell=q}^{\infty} c_\ell(x)\psi_\ell. \tag{20}$$

Thus, the localization information is carried by the first harmonic component not included in the fitted directivity model.

2.1.1. Monopole model

The monopole model is

$$m_1 = a_0\psi_0. \tag{21}$$

The fitted amplitude absorbs the monopole coefficient, namely

$$a_0 = c_0(x). \tag{22}$$

The leading residual term is therefore

$$R_1(x) = Akx\,\psi_1 + O(x^2). \tag{23}$$

Thus, the first residual term is linear in x.

2.1.2. Monopole-dipole model

The monopole-dipole model is

$$m_2 = a_0\psi_0 + a_1\psi_1. \tag{24}$$

The fitted amplitudes absorb the monopole and dipole coefficients:

$$a_0 = c_0(x), \qquad a_1 = c_1(x). \tag{25}$$

The leading residual term is therefore

$$R_2(x) = A\frac{k^2x^2}{4}\psi_2 + O(x^3). \tag{26}$$

Thus, the first residual term is quadratic in x.

2.1.3. Monopole-dipole-quadrupole model

The monopole-dipole-quadrupole model is

$$m_3 = a_0\psi_0 + a_1\psi_1 + a_2\psi_2. \tag{27}$$

The fitted amplitudes absorb the monopole, dipole, and quadrupole coefficients:

$$a_0 = c_0(x), \qquad a_1 = c_1(x), \qquad a_2 = c_2(x). \tag{28}$$

The leading residual term is therefore

$$R_3(x) = A\frac{k^3x^3}{24}\psi_3 + O(x^4). \tag{29}$$

Thus, the first residual term is cubic in x. These three cases show that increasing the order of the directivity model shifts the localization information toward higher powers of the source displacement.

3. Numerical validation

This section presents a Monte Carlo simulation used to validate the analytical behavior described in the previous sections. The objective is to show how the distribution of the estimated source position changes when the order of the fitted directivity model is increased.

3.1. Simulation setup

A circular array of $N_m = 100$ microphones is considered. The microphones are uniformly distributed on a circle of radius $R = 10$ m. The m-th microphone position is denoted by (X_m, Y_m). The true source is located at the reference position, chosen as the origin,

$$x^\star = 0, \qquad y^\star = 0. \tag{30}$$

The true source is a pure monopole with amplitude $a_0 = 1$. All higher-order multipole amplitudes are set to zero. Therefore, the simulated measured field is

$$\mathbf{y} = a_0\mathbf{d}_0(x^\star, y^\star) + \boldsymbol{\varepsilon}, \tag{31}$$

where $\mathbf{d}_0(x^\star, y^\star) \in \mathbb{C}^{N_m}$ is the complex monopole field generated by the true source position and evaluated at the microphone positions. Its m-th component is defined by

$$[\mathbf{d}_0(x^\star, y^\star)]_m = H_0(kr_m^\star), \tag{32}$$

where

$$r_m^\star = \sqrt{(X_m - x^\star)^2 + (Y_m - y^\star)^2}. \tag{33}$$

Since the true source is located at the center of the circular array, one has $r_m^\star = R$ for all microphones, and therefore $[\mathbf{d}_0(x^\star, y^\star)]_m = H_0(kR)$.

The vector $\boldsymbol{\varepsilon} \in \mathbb{C}^{N_m}$ is an additive complex noise vector. In the simulation, the real and imaginary parts of each noise component are independent Gaussian variables with standard deviation $\sigma = 10^{-3}$. More precisely,

$$\varepsilon_m = \sigma(\xi_m + \mathrm{i}\eta_m), \tag{34}$$

where ξ_m and η_m are independent standard normal variables. Therefore, the noise power per microphone is $2\sigma^2$. The frequency is $f_0 = 1000$ Hz and the sound speed is $c = 343$ m/s. Using the noiseless monopole field $H_0(kR)$, with $k = 2\pi f_0/c$, the corresponding signal-to-noise ratio is approximately $\mathrm{SNR}_{\mathrm{dB}} \simeq 32.4$ dB.

The source position is estimated on a one-dimensional search grid along the line $y = 0$. The grid is defined over the search interval

$$x_g \in [-0.03, 0.03], \tag{35}$$

using 5000 grid points. The interval is chosen to be local with respect to the acoustic wavelength. The wavelength is $\lambda = c/f_0 = 0.343$ m. The maximum searched displacement is therefore 0.03 m $\simeq 0.087\lambda$, meaning that the search interval corresponds to only about 8.7% of one wavelength. This confirms that the numerical search is restricted to small displacements around the reference position, consistently with the local Taylor expansion used in the analytical derivation. The grid coordinate x_g represents a candidate displacement around the reference position. Thus, the true displacement is zero, but the likelihood is evaluated over the grid of candidate positions. For each Monte Carlo trial, a new noisy measurement vector is generated and the source position is estimated on the grid.

3.2. Fitted multipole dictionary

For a candidate source position $(x_g, 0)$, the complex field associated with multipole order ℓ is represented by the vector $\mathbf{d}_\ell(x_g) \in \mathbb{C}^{N_m}$. Its m-th component is written as

$$[\mathbf{d}_\ell(x_g)]_m = H_\ell(kr_{g,m}) \exp(\mathrm{i}\ell\phi_{g,m}), \tag{36}$$

where the quantities $r_{g,m}$ and $\phi_{g,m}$ are respectively the distance and angle between the candidate source position and microphone m.

For a maximum multipole order K, the fitted dictionary is

$$D_K(x_g) = [\mathbf{d}_{-K}(x_g), \ldots, \mathbf{d}_0(x_g), \ldots, \mathbf{d}_K(x_g)]. \tag{37}$$

Thus, $D_K(x_g) \in \mathbb{C}^{N_m \times (2K+1)}$, and the fitted multipole amplitudes are complex-valued.

Although the analytical derivation is written using real cosine harmonics for simplicity, the numerical dictionary is expressed in terms of complex exponentials. This is the natural representation in a frequency-domain formulation, where acoustic pressure fields are described by complex phasors. Moreover, it allows the positive and negative multipole orders to be included symmetrically in the fitted dictionary.

Thus, the three tested cases are:

- $K = 0$: monopole model,
- $K = 1$: monopole-dipole model,
- $K = 2$: monopole-dipole-quadrupole model.

For each candidate position, the complex multipole amplitudes are estimated by least squares,

$$\widehat{\mathbf{a}}(x_g) = D_K(x_g)^+\mathbf{y}. \tag{38}$$

Here, $D_K(x_g)^+$ denotes the Moore–Penrose pseudo-inverse of the dictionary.

3.3. Profiled maximum likelihood criterion

For a fixed candidate position x_g, the fitted field is

$$\widehat{\mathbf{y}}(x_g) = D_K(x_g)\widehat{\mathbf{a}}(x_g). \tag{39}$$

The profiled least-squares criterion consists in minimizing the squared complex Euclidean norm (the squared ℓ_2-norm) of the residual,

$$\|\mathbf{y} - \widehat{\mathbf{y}}(x_g)\|_2^2. \tag{40}$$

Here, $\|\cdot\|_2$ denotes the Euclidean norm on complex vectors.

Equivalently, since $\|\mathbf{y}\|_2^2$ is independent of x_g, the estimator can be obtained by maximizing the projection energy,

$$B_K(x_g) = \left\|D_K(x_g)D_K(x_g)^+\mathbf{y}\right\|_2^2. \tag{41}$$

The estimated source position is therefore

$$\widehat{x} = \arg\max_{x_g} B_K(x_g). \tag{42}$$

3.4. Monte Carlo results

The simulation is repeated over 1000 independent noise realizations. For each realization, the source position is estimated using the profiled projection criterion. The resulting histograms of $\widehat{x}$ are shown in Fig. 1 for $K = 0$, $K = 1$, and $K = 2$.

The interpretation of these histograms can be clarified by comparison with simple (toy) scalar Gaussian mean models. This scalar comparison is only used to interpret the estimator distributions; the acoustic simulations themselves are performed with complex-valued pressure data. Let Y_i denote the i-th scalar observation in such a toy model. The data are assumed independent and distributed as

$$Y_i \sim \mathcal{N}(\mu_p(z), \sigma^2), \tag{43}$$

where z is the unknown scalar parameter, $\mu_p(z)$ is the mean function, and p denotes the power of this mean function. In the three cases considered here,

$$\mu_1(z) = z, \qquad \mu_2(z) = z^2, \qquad \mu_3(z) = z^3. \tag{44}$$

The true value is $z^\star = 0$. Therefore, in all three toy models, the generated data satisfy

$$Y_i \sim \mathcal{N}(0, \sigma^2). \tag{45}$$

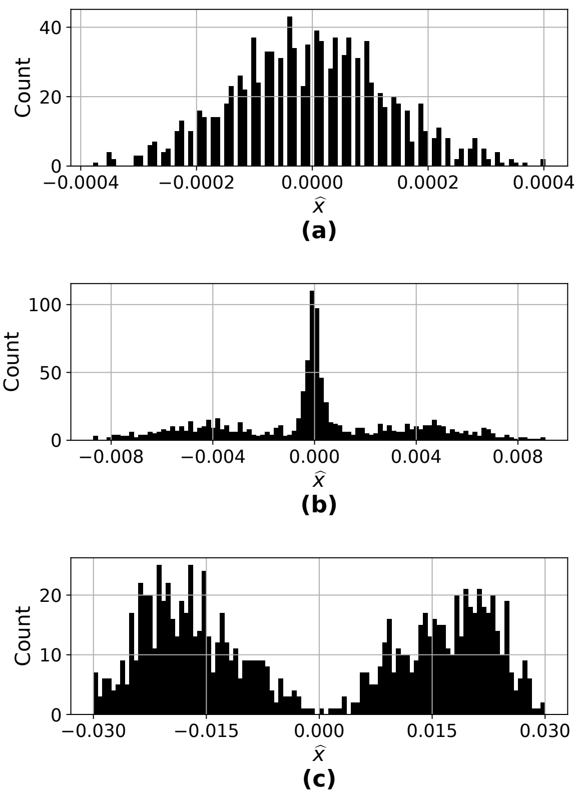

Figure 1: Monte Carlo histograms of the estimated source position for: (a) monopole model ($K = 0$), (b) monopole-dipole model ($K = 1$), and (c) monopole-dipole-quadrupole model ($K = 2$).

However, the estimator distribution is different in each case because the model used to infer z has a different mean function.

Let $\overline{Y}$ denote the sample mean. For the regular linear model, $Y_i \sim \mathcal{N}(z, \sigma^2)$, the maximum likelihood estimator is $\widehat{z} = \overline{Y}$, which is Gaussian. For the quadratic singular model, $Y_i \sim \mathcal{N}(z^2, \sigma^2)$, the estimator is obtained from $z^2 = \overline{Y}$, leading to zero or two symmetric maximizers depending on the sign of $\overline{Y}$. For the cubic singular model, $Y_i \sim \mathcal{N}(z^3, \sigma^2)$, the estimator is $\widehat{z} = \sqrt[3]{\overline{Y}}$, which produces a symmetric bimodal distribution with zero density at $\widehat{z} = 0$.

The acoustic simulations show the same qualitative statistical behavior because, after profiling the fitted multipole amplitudes, the first non-absorbed residual term scales linearly with x for $K = 0$, quadratically with x for $K = 1$, and cubically with x for $K = 2$, as shown in Eqs. (23), (26), and (29), respectively.

For $K = 0$, only the monopole amplitude is fitted. The first residual term is then proportional to the candidate displacement x_g. The estimation problem is regular and the estimated position asymptotically follows a Gaussian law centered around the true position. This is in agreement with the analytical prediction obtained from the scalar Gaussian linear mean model.

For $K = 1$, the monopole and dipole amplitudes are fitted jointly with the source position. The dipole contribution generated by a small candidate displacement can therefore be absorbed by the fitted directivity model. The leading residual term is then proportional to x_g^2. This creates a singular estimation problem. In the histogram, this appears as a strong concentration near $x = 0$, together with symmetric spreading on both sides of the true position. This is in agreement with the analytical prediction obtained from the scalar Gaussian quadratic mean model.

For $K = 2$, the monopole, dipole, and quadrupole amplitudes are fitted. In this case, both the linear and quadratic displacement signatures are absorbed by the directivity model. The first remaining residual term is proportional to x_g^3. The resulting estimator distribution is no longer Gaussian and becomes bimodal, with two symmetric peaks on both sides of the true reference position. This is in agreement with the analytical prediction obtained from the scalar Gaussian cubic mean model.

These numerical results confirm the theoretical analysis. Increasing the order of the fitted directivity model progressively removes the lower-order displacement information from the residual field. As a consequence, the localization problem becomes increasingly singular and the distribution of the estimated position changes from a standard unimodal shape to non-standard singular distributions.

4. Conclusions

This paper investigated the effect of joint position and directivity estimation on acoustic source localization. The analysis showed that, when multipole amplitudes are estimated freely, some displacement-induced field components can be absorbed by the fitted directivity model. As a consequence, the localization information is carried by the first residual harmonic that is not included in the model. For a monopole-only model, the leading residual term is linear in the candidate displacement, and the localization problem remains regular. This case has the same local structure as estimating a scalar parameter from a Gaussian mean model with a linear mean. When dipole or quadrupole components are included in the fitted model, the leading residual term becomes quadratic or cubic in the displacement. These cases are locally analogous to Gaussian mean models with quadratic and cubic means, respectively. At the reference source position, the corresponding first-order sensitivity vanishes, the Fisher information becomes singular, and the estimator distribution becomes non-standard. The numerical simulations confirmed these analytical predictions. With the true source located at the reference position, increasing the multipole order changed the distribution of the estimated position from the classical regular behavior, which is asymptotically Gaussian, to singular non-Gaussian distributions. These results highlight a trade-off in multipole-based acoustic localization: increasing the directivity model order can improve field representation, but it can also reduce the amount of independent information available for estimating the source position. The proposed analysis provides a theoretical explanation of this effect and clarifies how joint estimation of localization and directivity can degrade localization accuracy.

5. Acknowledgments

This work was supported by the Paris-Saclay Institute of Aeronautics and Astronautics (PSIA2) and the Graduate School of Engineering and Systems Sciences (GS SIS) of Université Paris-Saclay.

References

[1] G. Chardon, "Maximum likelihood estimators and cramér–rao bounds for the localization of an acoustical source with asynchronous arrays," *Journal of Sound and Vibration*, vol. 565, p. 117 906, 2023, ISSN: 0022-460X. DOI: https://doi.org/10.1016/j.jsv.2023.117906

[2] Y. Zhou, M. A. Diaz, D. Marx, R. Marchiano, C. Prax, and V. Valeau, "Localizing aeroacoustic sources in complex geometries: A hybrid method coupling 3d microphone array and time-reversal," *Journal of Sound and Vibration*, vol. 584, p. 118 452, 2024, ISSN: 0022-460X. DOI: https://doi.org/10.1016/j.jsv.2024.118452

[3] H. Demontis, F. Ollivier, and J. Marchal, "Block-sparse approach for the identification of complex sound sources in a room," in *EAA Spatial Audio Signal Processing Symp.*, Paris, France, Sep. 2019, pp. 13–17. DOI: 10.25836/sasp.2019.17

[4] M. N. Albezzawy, J. Antoni, and Q. Leclère, "The maximally-coherent reference technique and its application to sound source extraction without synchronous measurements," *Journal of Sound and Vibration*, vol. 599, p. 118 896, 2025, ISSN: 0022-460X. DOI: https://doi.org/10.1016/j.jsv.2024.118896

[5] M. Jones, T. Rogers, K. Worden, and E. Cross, "A bayesian methodology for localising acoustic emission sources in complex structures," *Mechanical Systems and Signal Processing*, vol. 163, p. 108 143, 2022, ISSN: 0888-3270. DOI: https://doi.org/10.1016/j.ymssp.2021.108143

[6] E. Monier and G. Chardon, "Cramér-rao bounds for the localization of anisotropic sources," in *2017 IEEE International Conference on Acoustics, Speech and Signal Processing (ICASSP)*, New Orleans, LA: IEEE, Mar. 2017, pp. 3281–3285, ISBN: 978-1-5090-4117-6. DOI: 10.1109/ICASSP.2017.7952763